CORRELATION OF ERTS MSS DATA AND EARTH COORDINATE SYSTEMS

William A. Malila
Ross H. Hieber
Arthur P. McCleer

August 1973

193300-18-SA/J

Prepared for presentation at Purdue Conference on Machine Processing of Remotely Sensed Data, October 16-18, 1973.

ENVIRONMENTAL
RESEARCH INSTITUTE
OF MICHIGAN
FORMERLY WILLOW RUN LABORATORIES,
THE UNIVERSITY OF MICHIGAN

CORRELATION OF ERTS MSS DATA AND EARTH COORDINATE SYSTEMS*

William A. Malila, Ross H. Hieber and
Arthur P. McCleer

Environmental Research Institute of Michigan (ERIM)**
Ann Arbor, Michigan

I. ABSTRACT

Experience has revealed a problem in the analysis and interpretation of ERTS multispectral scanner (MSS) data. The problem is one of accurately correlating ERTS MSS pixels with analysis areas specified on aerial photographs or topographic maps for training recognition computers and/or evaluating recognition results. It is difficult for an analyst to accurately identify which ERTS pixels (picture elements) on a digital image display belong to specific areas and test plots, especially when they are small.

A computer-aided procedure to correlate coordinates from topographic maps and/or aerial photographs with ERTS data coordinates has been developed. In the procedure, a map transformation from Earth coordinates to ERTS scan line and point numbers is calculated using selected ground control points and the method of least squares. The map transformation is then applied to the Earth coordinates of selected areas to obtain the corresponding ERTS point and line numbers. An optional provision allows moving the boundaries of the plots inwards by variable distances (typically $\geq$ half a resolution element) so the selected pixels will not overlap adjacent features.

II. INTRODUCTION

The computer-compatible-tape (CCT) form of ERTS-1 MSS data is well suited to analysis and recognition processing on digital computers. Examples of varied applications were reported by a number of investigators at the Goddard Space Flight Center's "Symposium on Significant Results from ERTS-1 Data" in March, 1973.

It is desirable to evaluate the accuracy of large-area resource surveys made by computer processing of ERTS, or other remote sensor, data. Such evaluations require the checking of recognition results for areas whose identities are known from field observations or other "ground truth" information sources. Even before recognition processing, the training of the classifiers usually involves the use of other areas of known identity that can be located in the remote sensor data.

The location of specific areas and assignment of pixels to individual fields and plots is more of a problem in ERTS data than in airborne scanner data which have finer spatial resolution. For instance, there are less than 600 ERTS pixels per square mile and a maximum of 18*** wholly

*This work was supported under ERIM Contract NAS5-21783 and an ERIM subcontract under Michigan State University Contract NAS5-21834.

**Formerly Willow Run Laboratories of The University of Michigan.

***Even this number is optimistic because the ERTS scan lines do not generally follow field boundaries. Further, as discussed under Section III, the oversampling along ERTS scan lines means that there is overlap between the areas viewed by the scanner for adjacent pixels and thus one must move away from boundaries to eliminate their effects.

within the boundaries of a 20-acre field. Section and field boundaries are frequently indistinct on ERTS data displays; consequently, errors are made in the visual location of fields and the subsequent assignments of pixels. Pixel misassignments potentially can cause errors in classification results and lead to incorrect conclusions. Even if detected, additional resources are required to correct errors.

ERTS images of two types are produced by the National Data Processing Facility at NASA/Goddard — system-corrected images and precision-processed images. They both represent photo maps but with different degrees of accuracy. The system-corrected images are corrected for the major distortions introduced by spacecraft orientation, sensor characteristics, and Earth's rotation. Precision-processed images include additional adjustments based on a number of in-scene ground-control points in each frame.

The bulk digital computer-compatible tape (CCT) data, however, are not corrected for any of these distortions. (Bulk data are preferred to precision CCT data for recognition processing because in the latter, the radiometric accuracy of the data is degraded by re-scanning.) Therefore, when displayed on a line-printer gray-tone map or CRT, substantial distortions are evident in bulk CCT data. Square sections are displayed as parallelograms, and other distortions are present. These distortions increase the difficulty of assigning pixels to specific ground areas, but the major cause of difficulty is the relatively large instantaneous field of view of the MSS scanner.

The problem of correctly assigning ERTS pixels to specific areas is somewhat different from two related problems which are under investigation elsewhere [Refs. 1-6]. Some investigators are studying the cartographic aspects of ERTS data, e.g., image quality and techniques to digitally correct ERTS data to match an Earth coordinate system, using spacecraft attitude information and/or ground control points spread throughout a frame. Others are studying the spatial registration of data from two or more frames that cover the same scene, using ground control points and/or image correlation techniques. The cartographic studies will simplify pixel assignments for areas that are readily identified by their latitude and longitude coordinates, but do not directly address procedures for assigning pixels for areas that are only identifiable on aerial photographs. The spatial registration studies will expedite the transfer of field coordinates from one frame to the next, but again do not consider the problem of initially assigning pixels to fields and test plots.

Techniques for both cartographic correction and spatial registration of ERTS data move data values from their original positions to an overlying grid by nearest-neighbor or interpolation rules. Then, the assignment of pixels to specific fields and test plots can take place; operations on a nearest-neighbor basis increase the uncertainty of true field boundary locations, while interpolation degrades radiometric fidelity. The procedure we have developed warps Earth coordinates to match ERTS coordinates, effectively computing the location of each pixel, and makes pixel assignments without any movement or interpolation of ERTS data.

III. PROCEDURE

The procedure described here for the computer-aided assignment of ERTS pixels relies on an empirical map transformation derived by least squares calculations from a local network of control points in and around the area of interest, e.g., a 20 x 25-km area on a 15' quadrangle map. These control points can be located on topographic maps and/or on aerial photographs. Differing scales can be handled, and the locations of control points and analysis areas on the maps and/or photographs can be obtained on a relative basis.

The empirical transformation produces rotations to account for the non-polar orbit of ERTS and the difference in orientation between Earth and ERTS-data coordinates, and also corrects for effects of the Earth's rotation and other sources of distortion and error, in a least-squares manner. The distortions in ERTS imagery are discussed in the Appendix and, for purposes of illustration only, two transformation matrices are computed: (1) a theoretical transformation that considers the major effects in ERTS data and (2) a similar transformation obtained by scaling the corresponding empirical Earth-to-ERTS coordinate transformation. Good, but not exact, agreement is shown between the two transformation matrices.

As noted earlier, we developed our computer-aided procedure because it is often difficult to distinguish "by eye" the corners of sections, fields, and plots of interest on digital displays of ERTS data, and more difficult to locate them accurately. Lack of contrast between materials and any banding or striping in the ERTS data can complicate matters. On the other hand, there generally are some road intersections and other features in the scene around and within the areas of interest that can be distinguished readily in digital displays.

In our procedure, we typically select fifteen to twenty distinguishable points as control points and estimate their ERTS line and point numbers as well as possible by inspection. Earth coordinates for the same points are determined* from a topographic map or an aerial photograph. A least-squares fit of Earth to ERTS coordinates reduces the error in the estimated location of each control point and produces a map transformation:

$$\begin{bmatrix} P \\ L \end{bmatrix} = \begin{bmatrix} a_{11} & a_{12} \\ a_{21} & a_{22} \end{bmatrix} \begin{bmatrix} X \\ Y \end{bmatrix} + \begin{bmatrix} b_1 \\ b_2 \end{bmatrix}$$

where P and L are the ERTS data coordinates for points along scan lines and for scan lines, respectively,

$\{a_{ij}\}$ are the empirical transformation coefficients,

X and Y are the Earth coordinates to be transformed,

and b_1 and b_2 are the offset parameters to account for different origins.

(A polynomial transformation has been computed but, thusfar, we have found that terms of higher than first order are not significant.)

The above transformation then is used to transfer Earth coordinates of other points, fields, or plots in the vicinity to their corresponding ERTS coordinates. For several purposes, it has been found convenient to place pixel designation information in a fifth channel added to ERTS data.

A companion computer program allows us to define each training or test area by a polygon with an arbitrary number (≤ 63) of vertices and to compute which ERTS pixel centers lie within the polygon. Further, there is a capability to move the polygon sides in or out by specified distances so as to include or exclude pixels whose signal values include effects of boundaries between scene features, for example, to avoid training on pixels that represent more than one material. An illustration of the effect of this procedure is presented in Figure 1. A section (1 mile square) in actual ERTS data was arbitrarily divided into 16 40-acre "fields". Part(a) of Figure 1 displays as blanks the pixels selected for these fields when the acceptance polygon was inset by one-half a resolution element on all sides.** An average of 22 pixels was selected for each 40-acre field. For Part(b), the inset was increased to three-quarters of a resolution element, and the smaller number of acceptable pixels (an average of 16) in each field is apparent. Parts(c) and (d) show the further reduction in the average number of acceptable pixels to 12 and 5 when the inset is increased to 1 and 1.5 resolution elements, respectively. Figure 2 presents other sets of "fields" delineated by the 0.5 resolution element criterion; field sizes of 640, 160, 80, and 10 acres are shown.

As noted above, the inset of one-half a resolution element is the theoretical minimum needed to exclude pixels whose radiometric signals contain boundary effects. A greater inset probably should be used in practice because of possible errors in the location of the control points in both the ERTS and Earth coordinates and in the location of test plot vertices in the maps or photographs. There also are known displacements inherent in the ERTS data which we presently do not explicitly take into account, e.g., the multiplexer delay in the spacecraft which introduces a displacement between the six scan lines in each mirror sweep.

IV. APPLICATION

A relatively large number of training and test fields were identified manually for use in recognition processing of ERTS-1 data for an agricultural problem, before the computer-aided

---

*Digitization is facilitated by the use of an x-y digitizing machine.

**Note that the inset must be greater than one-half a pixel dimension along the scan line since the actual resolution element size is 79 x 79 m even though the sampling rate along the scan lines gives an effective pixel width of approximately 57 m.

procedure was developed. Errors in the assignment of pixels to a few fields were identified during the course of the processing. One particular example is presented here.

Section roads were not always clearly discernible and were not present along all sides of every section, so several section lines were placed on line printer maps by simple interpolation between more distinct roads. The section in question is located on a boundary between two townships and happens to be less than one mile long in the N-S direction. Partly because of the smaller size, the lower section boundary was initially placed below the true boundary. Figure 3a presents the original manual assignment of pixels for four fields; the correct section lines are shown on the line printer map (of ERTS Band 5) and the actual field boundaries, as obtained from an aerial photograph, are mapped on the right. Fields 21, 22, and 23 were originally mis-assigned by the analyst. After poor agreement was observed between recognition results and the assigned crop types, these field delineations were checked and revised manually.

After the computer-aided pixel assignment procedure was developed, it was used to assign pixels to these same fields with a 0.5 resolution element inset. The resulting pixel assignments are presented in Figure 3b. Note the apparent good agreement between the selected pixels and the field boundaries, for example, around the notch in the upper right-hand corner of Field 21 and middle of Field 22. In this example, a USGS topographical map served as the standard coordinate reference for several road intersections that were readily identified in the ERTS data. The derived transformation then was applied to the standard coordinates of the section corners to locate them accurately within the ERTS data. Field vertices were determined relative to these section corners in an aerial photograph taken at the time of the ERTS pass. These relative locations of field vertices then were transformed to ERTS coordinates and pixels were selected.

It is difficult to make a quantitative assessment of the accuracy of our procedure, because of the lack of an absolute knowledge of pixel locations. One attempt is presented and discussed below, using Gull Lake, in Kalamazoo and Barry Counties, Michigan, as imaged in Frame 1033-15580.

A lake was selected because there generally is a large contrast between land and water in ERTS Band 7, so that the accuracy of boundary locations can be assessed. Gull Lake is one of the largest in the area, has some distinctive shoreline features and an island, and is in a region for which topographic maps were on hand. Since the topographic maps are several years old, it is important that the water level in Gull Lake is regulated so as to maintain a fixed level.

Our goals were (1) to select only those pixels that were completely within the lake and (2) to determine whether map-based coordinates of the shoreline features could be accurately placed in the ERTS data. The results discussed below show that a good job was done in selecting only water pixels and that shoreline features were accurately placed around the lake.

Eighteen control points were selected from a 6 x 20 mile area with Gull Lake roughly at the center. None of the control points were on the Gull Lake shoreline and few were near it because of indistinct roads in the immediate vicinity. Latitude and longitude for these points were extracted from three different USGS maps of two different scales. Approximately 90 points along the shoreline of Gull Lake on the USGS map also were digitized for transformation to ERTS coordinates. An inset of +0.5 resolution elements was used along the major shoreline and -0.5 along the shoreline of the island at the South end of the lake. The negative inset, or outset, was necessary to exclude island shoreline points from the water, because the island was the area outlined.

The line printer map in Figure 4 presents the results of the Gull Lake analysis. Five gray levels are displayed, three for values determined by the procedure to be within the lake and two for those outside. The choice of symbols within each of these two groups was determined by the value of the signal in ERTS Band 7. Observation showed that open water points were all at levels of 5 or less, while the surrounding land was generally at levels of 12 or greater; intermediate values were found along the shoreline. For points determined to be within the lake by the procedure, the predominant darkest symbol (M over $) corresponds to the 1554 points with values ≤ 5, the intermediate symbol (X over =) corresponds to the 18 points with values of 6 or 7, and the lightest symbol (*) corresponds to points with values ≥ 8. Only 9 points with values >8 were said to be within the lake, and the highest of these values was 9. Since land values generally are ≥ 12, the lighter pixels included at most only partial land observations. Further some of them might even have been caused by the presence of weeds near the shore; current aerial photography is not available to check for the presence of weeds. In summary, <1% of the lake points, or <3% of the shoreline points, seem to have been misclassified as being open water.

On the other side of the computer shoreline, 93 points with values ≤ 5 were placed (symbol θ). These points correspond to open water values that were excluded from Gull Lake. This result was not unexpected since the shoreline is irregular and was approximated by a multi-sided polygon.

All shoreline undulations on the map were not followed exactly and vertices were chosen to exclude all land from the polygon, leaving some water areas on the outside. Vertices around the island were all placed in the water.

Upon comparing the ERTS data of Figure 4 to the USGS map on the right-hand side, one can see that the inlets and peninsulas around the lake are accurately positioned by the procedure. The average accuracy of positioning is clearly better than one pixel, but we have not quantitatively determined how much better. The results encourage use of the procedure for processing of ERTS data.

V. CONCLUSIONS

A computer-aided procedure has been developed which provides increased accuracy and consistency over manual techniques for assigning ERTS pixels to specific ground areas. It is flexible in that it permits the use of USGS topographic maps or aerial photographs or a combination of the two, in assigning pixels.

The delineation of specific fields and plots for training recognition computers and evaluating results is an important problem that has not been addressed directly by other investigators concerned with either the cartographic aspects of ERTS data or spatial registration of data sets collected at different times. The assignment of pixels before any spatial adjustment of the pixels is made minimizes errors in such assignments. The accuracy of the procedure remains to be established quantitatively, but the examples given indicate that an average accuracy substantially better than one pixel is achievable.

APPENDIX. GEOMETRIC CHARACTERISTICS OF ERTS DATA

This appendix discusses the geometric characteristics of ERTS-1 data so as to give the reader a better understanding of the empirical transformation described in Section III. The major geometric differences between Earth coordinates and the ERTS data coordinates can be described by the product of several linear transformation matrices, one for each of the major differences, which transforms Earth coordinates to ERTS coordinates. One theoretical transformation is computed below for ERTS-1 orbit parameters at a specific location and compared to a corresponding matrix obtained empirically for one of the examples presented in Section IV. In addition, some typical values for errors introduced by satellite motions are computed for a local area within an ERTS frame.

The assumption made throughout is that the Earth's surface in a local area of up to $\sim$ 20 x 20 km size can be considered to be a plane surface on which meridians are parallel to each other and perpendicular to lines of constant latitude. Such an assumption is commonly made for localized plane land surveys [7].

A.1. THEORETICAL TRANSFORMATIONS

The major geometric characteristics of ERTS-1 data are (1) its non-polar orbit, (2) the different orientation of its data coordinates from those of common Earth coordinates, and (3) the distortion caused by the Earth's rotation.

Because the plane of the ERTS-1 orbit is inclined slightly ($\sim 9^{\circ}$) from that of a perfect polar orbit, the satellite crosses meridians of longitude with increasing frequency as it approaches the poles. Also, the angle at which it crosses these meridians increases at the higher latitudes. Following Kratky [8], we define the nominal track of the satellite to represent the ERTS-1 location when the Earth's rotation effect is neglected. Correspondingly, there is a nominal heading of the satellite relative to the local meridian of longitude:

$$H_s = \sin^{-1}\left[\frac{\sin \varepsilon}{\cos \phi}\right] = \sin^{-1}\left[\frac{0.1583933}{\cos \phi}\right] \qquad (1)$$

where H_s = nominal satellite heading, measured clockwise from South,

ε = polar inclination of the orbit (9.114° for ERTS-1 [9]),

and ϕ = latitude of the satellite.

The Earth's rotation causes both the actual sub-satellite track to deviate from the nominal track and the actual heading to deviate from the nominal heading. Kratky (op. cit.) approximates the deviation in heading as follows:

$$H_e \doteq \tan^{-1}\left[\left(\frac{\omega_e}{\omega_s}\right)\cos\varepsilon\sin\rho\right] \tag{2}$$

where ω_e = angular velocity of the Earth,

ω_s = angular velocity of the satellite ($\omega_e/\omega_s = 0.071713$ for ERTS-1),

and ρ = orbital travel angle as measured southward from the vertex of the orbit ($\rho = \pi/2$ at equator).

or, since $\sin\rho = \dfrac{\sin\lambda_s}{\cos\phi} = \dfrac{\tan\varepsilon}{\tan H_s}$

$$H_e \doteq \tan^{-1}\left[\left(\frac{\omega_e}{\omega_s}\right)\cos\varepsilon\left(\frac{\sin\lambda_s}{\cos\phi}\right)\right] = \tan^{-1}\left[\left(\frac{\omega_e}{\omega_s}\right)\frac{\sin\varepsilon}{\tan H_s}\right] \tag{3}$$

where λ_s, the nominal longitude of the satellite, can be computed from the actual longitude, λ, and latitude, ϕ, by the following relationship:

$$\lambda_s = \lambda - \left(\frac{\omega_e}{\omega_s}\right)\cos^{-1}\left[\frac{\sin\phi}{\sin\varepsilon}\right] \tag{4}$$

The Earth's rotation causes a shift along lines of constant latitude, converting squares to acute parallelograms (with tops rotated counter-clockwise by the angle, H_e) in uncorrected ERTS data.

The geometric relationships between Earth coordinates and ERTS data coordinates in a localized area can be represented by the product of several transformation matrices:

$$\begin{bmatrix} P - P_o \\ L - L_o \end{bmatrix} = M_5 \cdot M_4 \cdot M_3 \cdot M_2 \cdot M_1 \begin{bmatrix} \lambda - \lambda_o \\ \phi - \phi_o \end{bmatrix} \tag{5}$$

where P is the point count coordinate along scan lines,

L is the scan line count coordinate along the satellite track,

P_o and L_o are the ERTS data coordinates of the reference point,

$M_1, \ldots, M_5$ are transformation matrices,

λ is longitude, measured positive to the West,

ϕ is latitude, measured positive to the North,

and λ_o and ϕ_o are the Earth coordinates of the reference point.

A representation of the major effects is given by the following transformation matrices for specific effects:

$$\begin{bmatrix} P - P_o \\ L - L_o \end{bmatrix} = \underbrace{\begin{bmatrix} \frac{1}{P_{scl}} & 0 \\ 0 & \frac{1}{L_{scl}} \end{bmatrix}}_{M_5} \underbrace{\begin{bmatrix} 1 & \tan H_e \\ 0 & \frac{1}{\cos H_e} \end{bmatrix}}_{M_4} \underbrace{\begin{bmatrix} -1 & 0 \\ 0 & -1 \end{bmatrix}}_{M_3} \underbrace{\begin{bmatrix} \cos H_s & \sin H_s \\ -\sin H_s & \cos H_s \end{bmatrix}}_{M_2} \underbrace{\begin{bmatrix} \lambda_{scl} & 0 \\ 0 & \phi_{scl} \end{bmatrix}}_{M_1} \begin{bmatrix} \lambda - \lambda_o \\ \phi - \phi_o \end{bmatrix} \tag{6}$$

M_1 converts minutes of latitude and longitude to a standard unit of length, like meters, for the given latitude.

M_2 rotates the Earth coordinate axes by an angle, H_s, so the ϕ' axis is parallel to the satellite track (assuming no Earth rotation at this point).

M_3 rotates the axes by an additional 180^o so the positive directions of the transformed λ and ϕ axes correspond to the positive directions of the P and L axes, respectively.

M_4 accounts for the distortion caused by the Earth's rotation.

M_5 converts length measurements from standard units to ERTS pixel units, e.g., P_{scl} = # standard units/pixel width.

If we multiply the three middle matrices of Equation (6), they reduce to:

$$(M_4M_3M_2)_{Theoretical} = \begin{bmatrix} -\cos H_s + \tan H_e \sin H_s & -(\sin H_s + \tan H_e \cos H_s) \\ \frac{\sin H_s}{\cos H_e} & -\frac{\cos H_s}{\cos H_e} \end{bmatrix} \tag{7}$$

A corresponding relationship can be computed from an empirical transformation, since the empirical matrix, M, can equal:

$$M = M_5M_4M_3M_2M_1 \tag{8}$$

Pre- and post-multiplying by inverses,

$$M_5^{-1}MM_1^{-1} = M_4M_3M_2 \tag{9}$$

Thus, the empirical version of $M_4M_3M_2$ is:

$$(M_4M_3M_2)_{Empirical} = \begin{bmatrix} P_{scl} & 0 \\ 0 & L_{scl} \end{bmatrix} \begin{bmatrix} m_{11} & m_{12} \\ m_{21} & m_{22} \end{bmatrix} \begin{bmatrix} \frac{1}{\lambda_{scl}} & 0 \\ 0 & \frac{1}{\phi_{scl}} \end{bmatrix} \tag{10}$$

$$= \begin{bmatrix} \left(\frac{P_{scl}}{\lambda_{scl}}\right) m_{11} & \left(\frac{P_{scl}}{\phi_{scl}}\right) m_{12} \\ \left(\frac{L_{scl}}{\lambda_{scl}}\right) m_{21} & \left(\frac{L_{scl}}{\phi_{scl}}\right) m_{22} \end{bmatrix} \tag{11}$$

A.2. COMPARISON OF THEORETICAL AND EMPIRICAL TRANSFORMATIONS

It is of interest to compare an empirical transformation matrix obtained from one of the examples discussed in Section IV and the corresponding theoretical matrix for effects of non-polar orbit and Earth's rotation.

Assume:

$$\phi = 42.4^{\circ}$$

$$\varepsilon = 9.114$$

$$\omega_e/\omega_s = 0.071713$$

Then:

$$H_s = 12.39^{\circ}$$

$$H_e = 2.94^{\circ}$$

and the matrix of Equation (7) becomes:

$$\begin{bmatrix} -0.9656 & -0.2650 \\ 0.2149 & -0.9780 \end{bmatrix} \tag{12}$$

The corresponding empirical transformation matrix, scaled as in Equation (11), is:

$$\begin{bmatrix} -0.9628 & -0.2682 \\ 0.2101 & -0.9712 \end{bmatrix} \tag{13}$$

It can be seen that the two matrices are in good agreement, but are not exactly the same. There are several possible reasons for the small differences present. They include:

(1) Spacecraft motions, such as yaw, pitch, and roll, and other sources of error are not included in the theoretical transformation.

(2) Nominal orbit parameters were used for the theoretical transformation.

(3) There are residual errors in the locations of the control points in ERTS data, although the use of least-squares techniques minimizes them.

(4) The factors used to scale the empirical matrix depend on an assignment of dimensions to the pixels, and the exact dimensions depend on the MSS mirror scan velocity (a non-constant function) and the sampling rate, among other factors. A 57 x 79 m pixel size was used here.

A.3. COMPUTATION OF TYPICAL ERRORS

The actual heading of the spacecraft ground track, neglecting satellite perturbations, is the sum of the nominal heading and the deviation due to Earth's rotation:

$$H = H_s + H_e \tag{14}$$

It can be seen from Equations (1) and (6) that H_s decreases with decreasing latitude while H_e increases. Therefore, the two effects tend to cancel and minimize the change in heading across a portion of an ERTS frame.

Across a typical 15' quadrant topographic map (~20 x 25 km) the net change in heading is small and results in a displacement that is small in comparison to an ERTS pixel size. The heading is a function of only latitude for a spherical Earth. In passing from 42°45'N to 42°30'N latitude, the change in actual ERTS-1 headings is calculated to be:

$$\Delta H = H_{42^{\circ}30'} - H_{42^{\circ}45'} = -0.0384^{\circ} = -2.3'$$

where $H_{42°30'} = 12.3092 + 2.9557 = 15.2649°$

and $H_{42°45'} = 12.3587 + 2.9445 = 15.3032°$

For an area 20 km wide, this amounts to a total differential displacement of 13 m due to heading change. Therefore, it is a good assumption that the spacecraft flies along a straight line over a local area ∿20 km wide.

Spacecraft motions also introduce additional variations during a pass over the same size area, ∿20 km x 25 km. If we consider differential angles of 0.13×10^{-3} rad for yaw, 0.20×10^{-3} rad for pitch, and 0.11×10^{-3} rad for roll, the corresponding differential displacements would be ∿3 m for yaw, 180 m for pitch, and 100 m for roll. Differential yaw and pitch affect the spacing of data primarily along the flight line, whereas roll affects it primarily along the scan line. Effects of such spacecraft motions are not included in the theoretical transformation described earlier, but are included in the empirical procedure used for pixel assignments which averages over them in a least-squares sense.

REFERENCES

(References 1-6 were presented at the "Symposium on Significant Results Obtained from ERTS-1", March 5-9, 1973, New Carrollton, Md., sponsored by NASA/Goddard Space Flight Center, Greenbelt, Md.)

1. McEwen, R. B., 1973. "Geometric Quality of ERTS-1 Images".

2. Rifman, S. S., 1973. "Digital Rectification of ERTS Multispectral Imagery".

3. Bernstein, R., 1973. "Results of Precision Processing (Scene Correction) of ERTS-1 Images Using Digital Image Processing Techniques".

4. Bauer, M. E., 1973. "Identification of Agricultural Crops by Computer Processing of ERTS MSS Data".

5. Billingsley, F. C. and A. F. H. Goetz, 1973. "Computer Techniques Used for Some Enhancement of ERTS Images".

6. Bizzell, R., L. Wade, H. Prior, and B. Spiers, 1973. "The Results of an Agricultural Analysis of ERTS-1 MSS Data at the Johnson Space Center".

7. Davis, Foote, and Kelly, 1966. Surveying: Theory and Practice, McGraw-Hill.

8. Kratky, Valadimir, 1972. "Photogrammetric Solution for Precision Processing of ERTS Images", presented at XII International Congress of Photogrammetry, Ottawa, Canada, July 1972.

9. ERTS Investigators" Bulletin, Vol. A, No. 4, 8 August 1972, NASA/GSFC, Greenbelt, Md.

Addition to paper, "CORRELATION OF ERTS MSS DATA AND EARTH COORDINATE SYSTEMS", by Malila, Hieber, and McCleer.

ACKNOWLEDGEMENT

The authors wish to acknowledge helpful discussions and suggestions by their colleagues, M. M. Spencer, H. M. Horwitz, and R. J. Kauth.

Note Added in Publication: R. Kauth has pointed out that Equation (7) can be reduced to:

$$(M_4M_3M_2)_{\text{Theoretical}} = \frac{1}{\cos H_e}\begin{bmatrix} -\cos H & -\sin H \\ \sin H_s & -\cos H_s \end{bmatrix} \qquad (7')$$

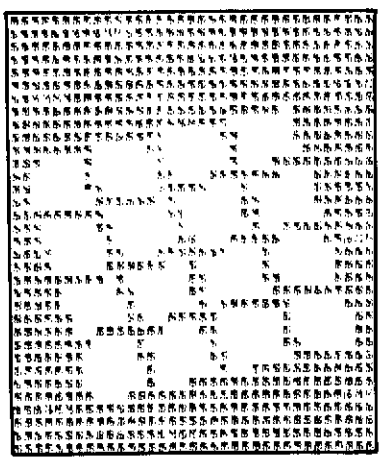

Part (a) 0.5 INSET

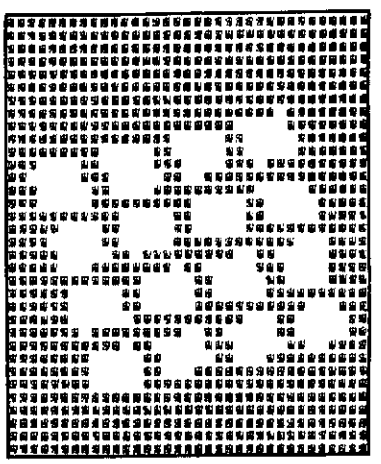

Part (b) 0.75 INSET

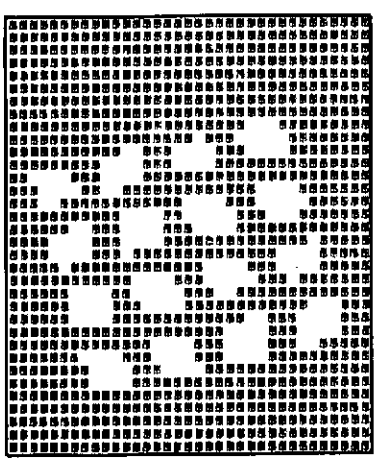

Part (c) 1.0 INSET

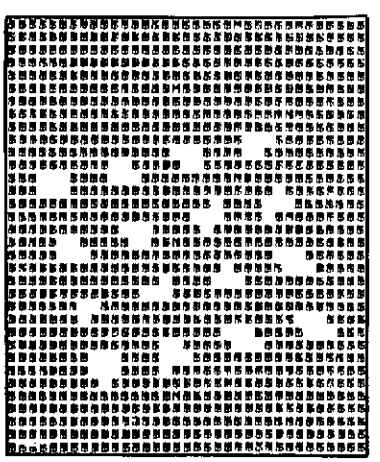

Part (d) 1.5 INSET

ERIM

EFFECT OF INSET PARAMETER ON PIXEL SELECTION FOR 40-ACRE FIELDS

(Inset Parameter is Measured in MSS Resolution Elements)

FIGURE 1

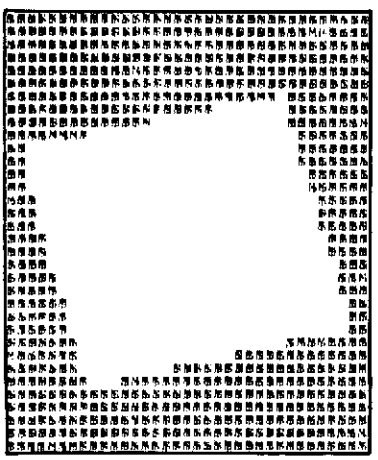

640 ACRE FIELD

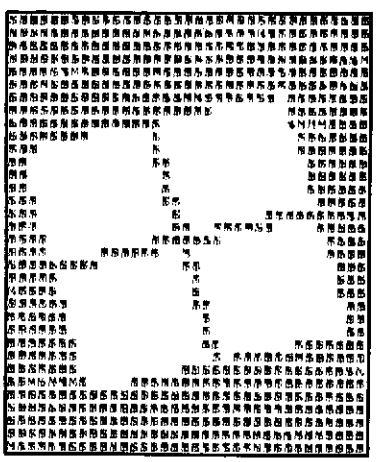

160 ACRE FIELDS

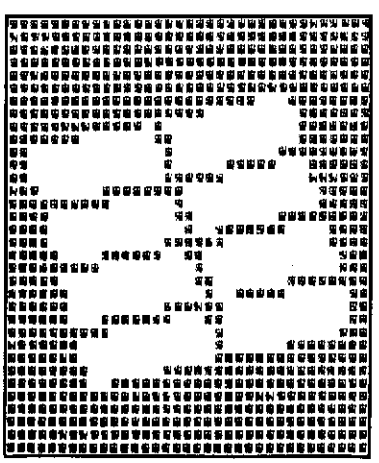

80 ACRE FIELDS

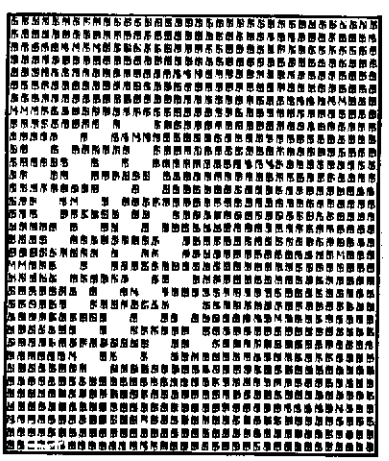

10 ACRE FIELDS

EFFECT OF FIELD SIZE ON PIXEL SELECTION FOR 0.5-RESOLUTION-ELEMENT INSET

ERIM

FIGURE 2

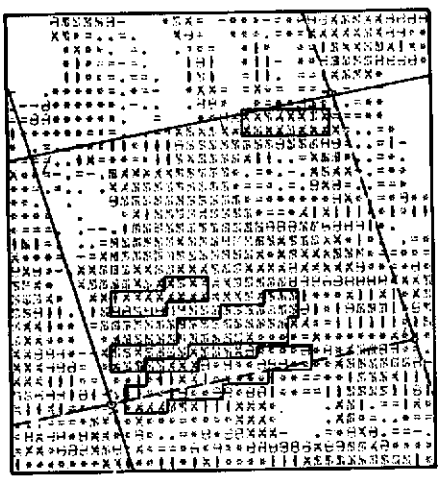

ORIGINAL MANUAL ASSIGNMENT

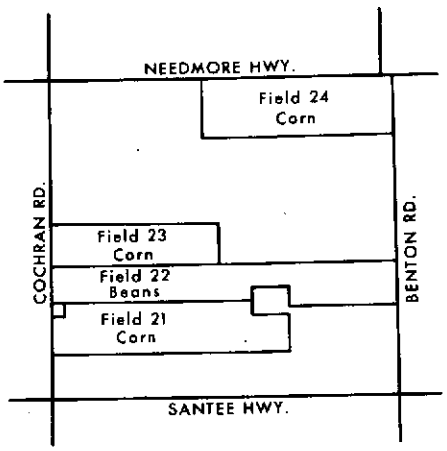

MAP OF FIELD BOUNDARIES

EXAMPLE OF FIELD LOCATION IN ERTS DATA

FIGURE 3a

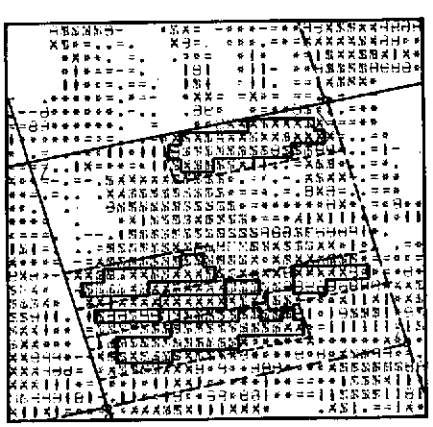

COMPUTER-AIDED ASSIGNMENT

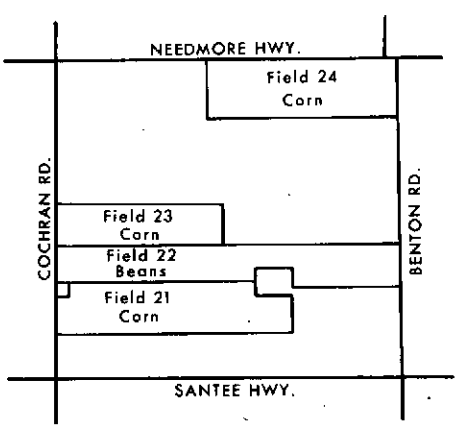

MAP OF FIELD BOUNDARIES

EXAMPLE OF FIELD LOCATION IN ERTS DATA

FIGURE 3b

ERIM

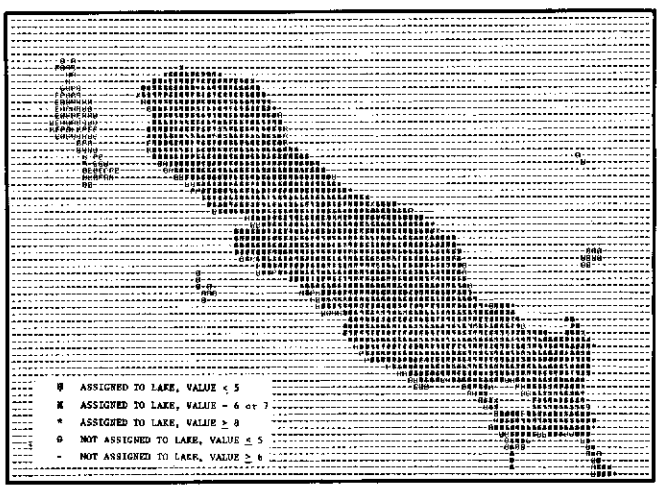

ERTS PIXEL ASSIGNMENT

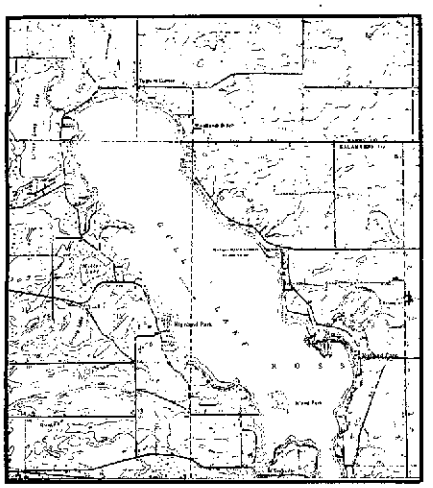

MAP OF GULL LAKE

RESULTS OF COMPUTED-AIDED ASSIGNMENT OF ERTS PIXELS TO OPEN WATER IN GULL LAKE

FIGURE 4

ERIM